

Received September 20, 2019, accepted October 5, 2019, date of publication October 9, 2019, date of current version October 22, 2019.

Digital Object Identifier 10.1109/ACCESS.2019.2946349

Sliding Mode Control for Permanent Magnet Synchronous Motor Drive Based on an Improved Exponential Reaching Law

AIMENG WANG AND SHENGJUN WEI 

School of Electrical and Electronic Engineering, North China Electric Power University, Baoding 071003, China

Corresponding author: Shengjun Wei (weishengjun1@163.com)

This work was supported in part by the Beijing Natural Science Foundation of China under Grant 3172037, and in part by the Natural Science Foundation of Hebei Province of China under Grant E2017502025.

ABSTRACT Permanent magnet synchronous motor (PMSM) is a typical nonlinear and multi-variable coupled system, which is sensitive to the uncertainty or variations in the motor parameters and the external disturbance which lead to the deterioration of the steady-state performance. Therefore, it is necessary to introduce effective control methods to improve the drive quality. In this paper, the DQ -axes inductances considering the magnetic saturation of the PMSM which has a significant influence on the operating characteristics are obtained, and the variable parameters are substituted into the control system. Then, a novel sliding mode control strategy is analyzed and adopted. An improved exponential reaching law is proposed in order to solve the chattering problem and improve the performance, which is verified by the theory and simulation. It demonstrates the smooth and quick responses using the new approach can be achieved to enhance the robustness of the drive system compared with conventional sliding mode control method.

INDEX TERMS Permanent magnet synchronous motor (PMSM), variable parameters, sliding mode control, improved exponential reaching law, drive performance.

I. INTRODUCTION

Permanent magnet synchronous motor (PMSM) has been widely used in many fields due to its high power density, high output torque and high efficiency [1]–[3].

PMSM is a typical nonlinear and multi-variable coupled system, the parameters such as flux linkage and DQ -axes inductances are varying due to the magnetic saturation in the actual motor operation, and the uncertainties caused by these variations have a great impact on the control performance. Furthermore, different temperatures or operating conditions in the external environment will also reduce the stability of the drive system. So it is necessary to adopt more advanced methods to solve the above problem.


Sliding mode control (SMC) strategy emerged at this historic moment to overcome this serious difficulty. Its remarkable advantage is that the structure of the SMC controller is not complicated but it has strong robustness to uncertain parameters and external disturbance, which has been

described in detail in [4]–[6]. Therefore, this algorithm has gradually become a widely used analytical method in various systems.

The performance of sliding mode control system largely depends on the design and selection of the sliding mode surface, and it has become a very important issue. There are two main types of sliding mode surfaces: linear sliding mode surface and non-linear sliding mode surface.

Linear sliding mode surface is the most common surface, it is a linear function of the system state. This control system is simple, convenient and the design of its parameters is relatively easy [7], [8]. However, its application in complex non-linear systems is inadequate. So many scholars are devoted to the study of the non-linear sliding mode surface, and have proposed many methods: piecewise linear sliding mode surface, terminal sliding mode [9]–[12] and integral sliding mode [13], [14].

Terminal sliding mode [9], [10] control can improve the convergence speed of the dynamic system, but this speed is slow when the system state is far from the equilibrium point, even far lower than linear sliding mode control.

The associate editor coordinating the review of this manuscript and approving it for publication was Ning Sun .

So Yu improved this method, and proposed fast terminal sliding mode (FTSM) [11] to try to achieve the optimal control in time. In addition, Feng Yong proposed a nonsingular terminal sliding mode (NTSM) [12] to solve the singularity problem. Integral sliding mode (ISM) control is another kind of non-linear SMC which is widely used. In the reaching movement stage, the integrator is added to eliminate the steady-state error. In [13], the robustness of ISM surface is analyzed and a design method based on the disturbance norm minimization is proposed. In [14], the adaptive ISM control is used to improve the control accuracy of PMSM. Although the ISM controller improves the robustness, it makes the system no longer have the reduced-order characteristics on the sliding mode surface, that is, its order is high and its calculation is complicated.

Nowadays, more and more experts are interested in the study of control laws. Among different reaching laws, the exponential reaching law is the most popular since it is easy to implement and control, while the chattering problem may exist [15]–[17]. So many scholars try to improve it, for example, Levant and Bartolini proposed a high-order SMC method to solve this question [18]–[20].

Some intelligent algorithms such as adaptive control [21], neural-network [22] and fuzzy control [23], are developing to eliminate the chattering as well in last several years. In [24], a neural network-based adaptive antiswing control method is used into the ship-mounted crane systems, which is novel and also applicable to this paper. In a word, SMC strategy is becoming more and more widespread in practical application.

In this paper, an interior PMSM is taken as the research object. The motor structure and magnetic flux distribution are obtained by finite element analysis as shown in FIGURE 1. This motor is able to operate steadily since the magnetic flux is symmetrical. Then, an improved exponential reaching law based on traditional sliding mode theory is applied into the motor control system. The superiorities of the proposed method are as follows:

1. It is simpler without too much complicated calculation compared with other improved SMC strategies.
2. The chattering is able to be suppressed well and the robustness is improved although the proposed method is still the first-order sliding mode.
3. The novel strategy is feasible and has better dynamic performance compared with conventional reaching law and PI method.

But, there are some difficulties encountered in practical application:

1. The magnetic saturation has a serious influence on the performance of the motor, such as the DQ -axes inductances are varying along with the currents. Therefore, it's important to find appropriate ways to solve this problem.

2. The proposed reaching law contains many cases, so its analysis and comparison with traditional methods are complicated. Lots of time is needed.

Based on the above shortcomings and advantages, a detailed introduction and research will be made in this paper.

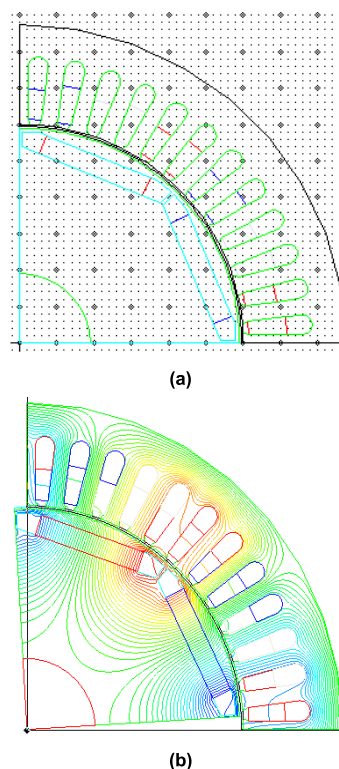


FIGURE 1. Cross sections of the structure and magnetic flux distribution of the studied PMSM. (a) Motor structure. (b) Magnetic flux distribution at no-load.

II. NOVEL SLIDING MODE CONTROL ALGORITHM

A. MODEL OF PMSM CONSIDERING MAGNETIC SATURATION

The motor studied is an interior PM motor, which has asymmetrical rotor structure, in other words, the magnetic circuits of the DQ -axes are asymmetrical. This motor is equivalent to a salient-pole motor and has a reluctance torque generated by the salient effect.

The effect of armature reaction magnetic field makes the reluctance change greatly, which results in serious magnetic saturation and affects the output of the reluctance torque. Because the D -axis is located in the axial position of the permanent magnet and the permeability of the permanent magnet is close to the permeability of air, the effective air gap of the D -axis is larger than that of the Q -axis. Besides, the reluctance of the Q -axis varies greatly. Therefore, the change of the Q -axis inductance (smaller air gap) with I_q is much larger than that of the D -axis inductance with I_d , that is, the influence of the magnetic saturation mainly exists in the Q -axis. The variations of inductances along with the currents are indicated in FIGURE 2.

In addition, after making some assumptions to simplify the calculation, such as: stator windings are symmetrical and identical; only sinusoidal wave flux potential is generated in the air gap when the stator currents are three-phase symmetrical sinusoidal currents and so on [25], we can get some essential equations. In DQ coordinate system, the voltage equations are shown in (1), and the differential term is 0 when

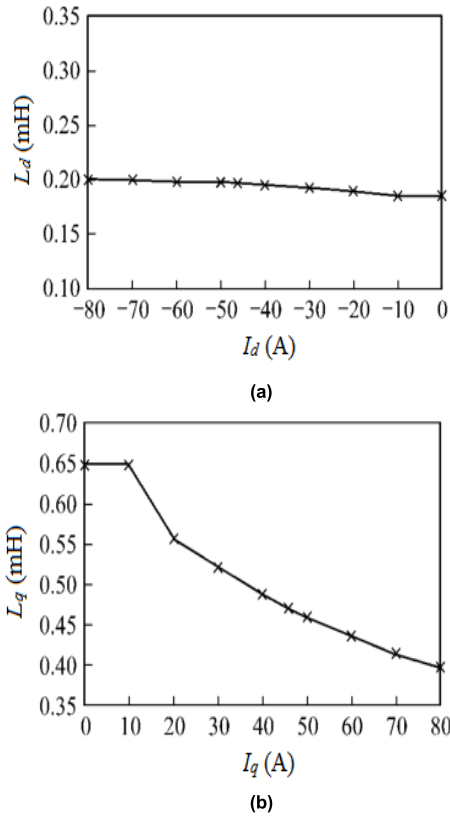


FIGURE 2. Variation of DQ-axes inductances versus DQ-axes currents. (a) D-axis inductance (L_d). (b) Q-axis inductance (L_q).

the motor is running in steady state, so we can get (2) by simplifying the differential term. Then the expression of the Q-axis inductance can be obtained as shown in (3). The torque and motion equations of the motor are shown in (4) and (5), respectively.

$$\begin{cases} u_d = Ri_d - \omega_e \hat{L}_q i_q + L_d \frac{di_d}{dt} \\ u_q = Ri_q + \omega_e (L_d i_d + \varphi_f) + \hat{L}_q \frac{di_q}{dt} \end{cases} \quad (1)$$

$$\begin{cases} u_d = Ri_d - \omega_e \hat{L}_q i_q \\ u_q = Ri_q + \omega_e (L_d i_d + \varphi_f) \end{cases} \quad (2)$$

$$\hat{L}_q = Ri_d - u_d / \omega_e i_q \quad (3)$$

$$T_e = \frac{3}{2} p [\varphi_f + (L_d - \hat{L}_q) i_d] i_q \quad (4)$$

$$T_e - T_L = \frac{J}{p} \frac{d\omega_m}{dt} \quad (5)$$

where u_q, u_d - the terminal voltages of the Q, D axes (V)
 i_q, i_d - armature current components (A)
 φ_f - permanent magnet flux (Wb), regarded as a constant
 \hat{L}_q, L_d - stator inductances (mH)
 R - winding resistance (Ω), regarded as a constant
 J - moment of inertia ($\text{kg}\cdot\text{m}^2$)
 p - number of pole pairs
 ω_e, ω_m - electrical and mechanical angular speed (rad/s)
 T_e, T_L - electromagnetic torque and load torque ($\text{N}\cdot\text{m}$)

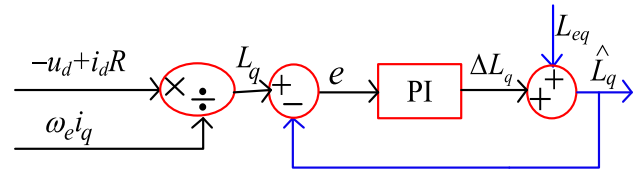


FIGURE 3. Self-regulatory model of the Q-axis inductance.

Some equations have changed from non-linearity to linearity under certain conditions. The purpose is very clear, that is, we try to reduce the calculation and facilitate the analysis as much as possible under the premise of less influence on the model. All of formulas provide a necessary theoretical basis for the realization of SMC method.

As can be seen from FIGURE 2, the D-axis inductance is regarded as a constant (0.20mH); but the Q-axis inductance varies greatly with the Q-axis current. So in order to improve the drive quality as much as possible, the varying Q-axis inductance needs to be input into the system. According to the basic idea of model identification, that is, the error is adjusted by an adaptive mechanism to make the dynamic process of the model as consistent as possible with the actual process [26]. The expression of the Q-axis inductance is presented in (6) and its self-regulatory model is established as seen in FIGURE 3.

$$\begin{aligned} \hat{L}_q &= \Delta L_q + L_{eq} = (L_q - \hat{L}_q) \left(K_p + \frac{K_i}{s} \right) + L_{eq} \\ &= \{ (Ri_d - u_d) / \omega_e i_q - \hat{L}_q \} \left(K_p + \frac{K_i}{s} \right) + L_{eq} \end{aligned} \quad (6)$$

L_{eq} is the rated Q-axis inductance. The parameters (u_d, i_d, i_q and ω_e) are changing when the motor is running. Then the varying Q-axis inductance is adjusted by the parameter adaptive mechanism, and finally we can get the variation of the Q-axis inductance which is similar to FIGURE 2. (b), then it is applied to the drive system.

What's more, the D-axis current is coupled with Q-axis current due to the existence of DQ-axes stator inductances and angular speed according to (2). So a voltage feed-forward compensation module is needed to eliminate the interaction between currents. After adding PI controllers to regulate current and a series of formula transformations, the given voltage of the decoupled DQ-axes can be obtained as shown in (7). The structure of the feed-forward module is shown in FIGURE 4. Inside it, the time-varying Q-axis inductance is taken to compensate the voltage for more precise control.

$$\begin{cases} u_d^* = \left(K_{pd} + \frac{K_{id}}{s} \right) (i_d^* - i_d) - \omega L_q i_q \\ u_q^* = \left(K_{pq} + \frac{K_{iq}}{s} \right) (i_q^* - i_q) + \omega (L_q i_q + \varphi_f) \end{cases} \quad (7)$$

Considering the effect of the magnetic saturation and properly simplifying the mathematical model of PMSM, the control method is simple but the drive performance can be improved.

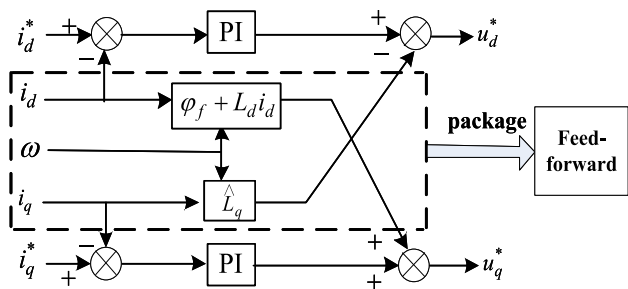


FIGURE 4. Voltage feed-forward decoupling module.

B. PROPOSED EXPONENTIAL REACHING LAW

According to the basic principle of SMC theory, various reaching laws can be designed to ensure the quality of the movement stage. Among them, the exponential reaching law is the most common and it will be studied in this paper.

The system state variables are defined as (8). And through the derivation, the expression of conventional exponential reaching law and the output of the controller (i.e. the given Q-axis current) are obtained, as shown in (9) and (10), respectively. *s* is the system sliding mode surface.

$$\begin{cases} e = x_1 = \omega_m^* - \omega_m \\ \dot{e} = x_2 = \frac{dx_1}{dt} = -\frac{d\omega_m}{dt} \end{cases} \quad (8)$$

$$\dot{s} = -m \text{sign}(s) - qs, \quad m > 0, q > 0 \quad (9)$$

$$i_{q^*} = \frac{1}{A} \int (cx_2 + m \text{sign}(s) + qs) dt \quad (10)$$

Based on the analysis of above traditional sliding mode theory, an improved exponential reaching law is proposed to enhance the dynamic performance of the drive system, as shown in (11).

$$\begin{cases} \dot{s} = -m |X|^a \text{sign}(s) - qs \\ \lim_{t \rightarrow \infty} |X| = 0, m > 0, q > 0, a \in \mathbb{N}^* \end{cases} \quad (11)$$

where *X* can take *x*₁, *x*₂ or *s*, that is, *X* is closely related to the state variables.

When the distance between the system state and the sliding mode surface is far, *X* is big and then the system state will reach the sliding mode surface by the $-m |X|^a \text{sign}(s)$ and $-qs$, so the reaching speed is improved; When the system state is near to the sliding mode surface, $-qs$ is close to zero and the $-m |X|^a \text{sign}(s)$ plays the main role. In a word, the increase of $|X|^a$ makes the state variables close to zero and stabilize at the origin more quickly, which can effectively suppress the chattering and improve the dynamic performance.

Definition: $A = 3p^2 \varphi_f / 2J$, $U = di_q/dt$. Combing (4), (5), (8), (11) and $i_d = 0$ control, we can get (12) and the new

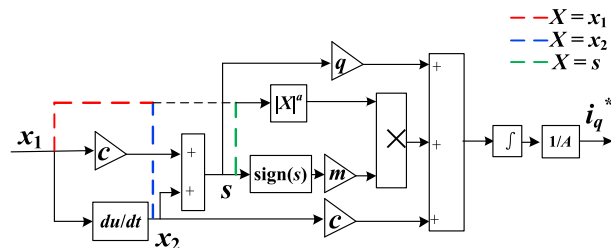


FIGURE 5. Internal structure of new sliding mode controller.

given current i_{q^*} is shown in (13).

$$\begin{cases} \frac{dx_1}{dt} = -\frac{d\omega_m}{dt} = -\frac{p}{J} (\frac{3}{2} p \varphi_f i_q - T_L) = x_2 \\ \frac{dx_2}{dt} = -\frac{d^2\omega_m}{dt^2} = -\frac{3p^2}{2J} \varphi_f \frac{di_q}{dt} = -AU \end{cases} \quad (12)$$

$$i_{q^*} = \frac{1}{A} \int (cx_2 + m |X|^a \text{sign}(s) + qs) dt \quad (13)$$

Three adjustable constants (*c*, *m*, *q*) in SMC controller are used instead of two adjustable parameters (*k_p*, *k_i*) in PI controller, which is more likely to improve the performance. After adjustment, we choose the appropriate value (*c*, *m*, *q*) to use. In this paper, these values are: *c* = 60; *m* = 200; *q* = 200.

According to the above Formulas, we can construct a new SMC controller as shown in FIGURE 5. The connection of three kinds of dotted lines represents the difference in the value of *X*. The red line represents *X* = *x*₁; the blue line represents *X* = *x*₂ and the green line represents *X* = *s*.

C. STABILITY ANALYSIS

Lyapunov function is often used to judge the stability of a linear or non-linear system. We select $V = s^2/2$ as the Lyapunov function. The accessibility condition of sliding mode must be satisfied in the normal motion stage as shown in (14), so that the state variables can reach the sliding mode surface in a finite time from any unknown initial state [27]. System sliding mode surface $s = cx_1 + x_2$, it satisfies two conditions: *s*(*x*) is a differentiable function and *s*(0) = 0.

$$\lim_{s \rightarrow 0^+} \dot{s} < 0, \lim_{s \rightarrow 0^-} \dot{s} > 0 \Rightarrow \dot{s}s < 0 \quad (14)$$

where $\dot{s} = ds(t)/dt$,

Combining Lyapunov stability theorem, the stability condition of sliding mode controller is:

$$V = \frac{1}{2} s^2 > 0 \& \dot{V} = \dot{s}s < 0 \quad (15)$$

It is obvious that *V* > 0 is valid; Bring (11) into (15) and the time derivative of the Lyapunov function is got:

$$\begin{aligned} \dot{V} &= \dot{s}s = s \{-m |X|^a \text{sign}(s) - qs\} \\ &= -m |X|^a |s| - qs^2 < 0 \end{aligned} \quad (16)$$

Sign (s) is a symbolic function that indicates whether the parameter is positive or negative. When $s > 0$, $\text{sign}(s) = 1$; $s = 0$, $\text{sign}(s) = 0$; $s < 0$, $\text{sign}(s) = -1$.

In some references, the function $\text{sign}(s)$ is defined as: when $s > 0$, $\text{sign}(s) = 1$; $s = 0$, $-1 \leq \text{sign}(s) \leq 1$; $s < 0$, $\text{sign}(s) = -1$.

From (14), we can know that the value of s is infinitely close to 0 in the positive and negative directions, but $s \neq 0$. Therefore, the equation (16) is always true because $|X|$ and the constants (a, m, q) are all larger than 0, and $s \neq 0$.

So even when $s = 0$, $-1 \leq \text{sign}(s) \leq 1$; it does not affect the stability of the system because it is not taken into account. But $\text{sign}(s)$ is 0 when $s = 0$ in this paper.

The equation (16) shows that the considered Lyapunov function satisfies the stability condition, that is, the theorem (15). So we conclude that the motor drive system using the improved sliding mode controller is stable.

Detailed performance analysis of the proposed reaching law will be made in the next section. The stability can also be seen from the analysis below.

III. PERFORMANCE OF THE IMPEOVED METHOD

The performance of the reaching laws themselves can best reflect their own intrinsic quality. X can take different values, so can a . These reaching laws will be introduced separately in this section.

A. $X=x_1$

The exponential reaching law at this time is shown as:

$$\dot{s} = -m|x_1|^a \text{sign}(s) - qs \quad (17)$$

For the convenience of drawing analysis, the original sliding mode control reaching law is defined as ‘‘SMC’’; When a is a large value, such as $a = 4$, the reaching law at this time is defined as ‘‘SMC NEW1’’ and its performance is shown in FIGURE 6. It can be seen that:

1. For the state variable x_1 , the reaching law named ‘‘SMC NEW1’’ falls slower and fluctuates more frequently when it comes to the steady state compared with ‘‘SMC’’.
2. Similarly, for the state variable x_2 , ‘‘SMC NEW1’’ also fluctuates more frequently.
3. The phase trajectory of ‘‘SMC NEW1’’ also has more frequent fluctuation which is harmful to motor operation.

In summary, the reaching law of ‘‘SMC NEW1’’ is not an appropriate reaching law because of its poor performance.

As the value of a increases, the fluctuation which is shown above increases. So we need to reduce the value of a . But when a is very small, $a = 1$, for example, the performance is almost unchanged compared with the original reaching law. So in order to improve the dynamic performance of the motor, a takes values 2 and 3 in this paper. When $a = 2$, this reaching law is defined as ‘‘SMC NEW2’’; the reaching law when $a = 3$ is defined as ‘‘SMC NEW3’’. The comparison of the performance curves of the three reaching laws are shown in FIGURE 7.

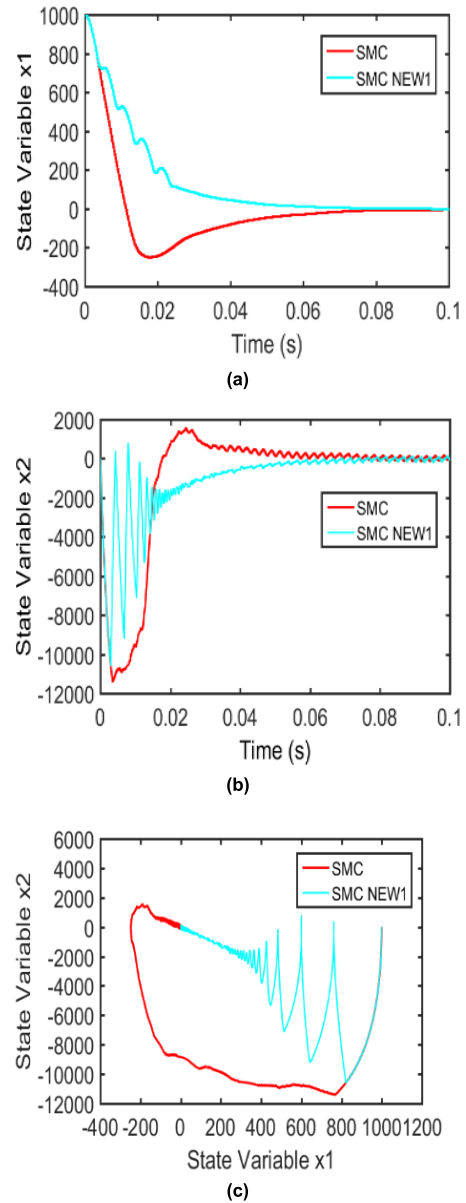


FIGURE 6. Comparison of the performance for two reaching laws when $X = x_1$. (a) Reaching speed. (b) State convergence process. (c) Phase trajectory.

We can know a lot from above figures:

1. For the state variable x_1 , the new reaching laws have smoother transition to the steady state; and especially ‘‘SMC NEW3’’ has no speed fluctuation as shown in FIGURE 7. (a).
2. As for the state variable x_2 , the maximum error at the start time of ‘‘SMC NEW3’’ is near 4000, while that of ‘‘SMC NEW2’’ and ‘‘SMC’’ are both bigger than 10000.
3. From FIGURE 7. (c), the two new reaching laws both have more regular phase trajectories; and ‘‘SMC NEW3’’ is the most regular and excellent one.

All in all, the new reaching law, especially ‘‘SMC NEW3’’, has the smoothest reaching speed; the speed fluctuation of the convergence process is smallest; and the phase trajectory is the most regular. So it can be regarded as the

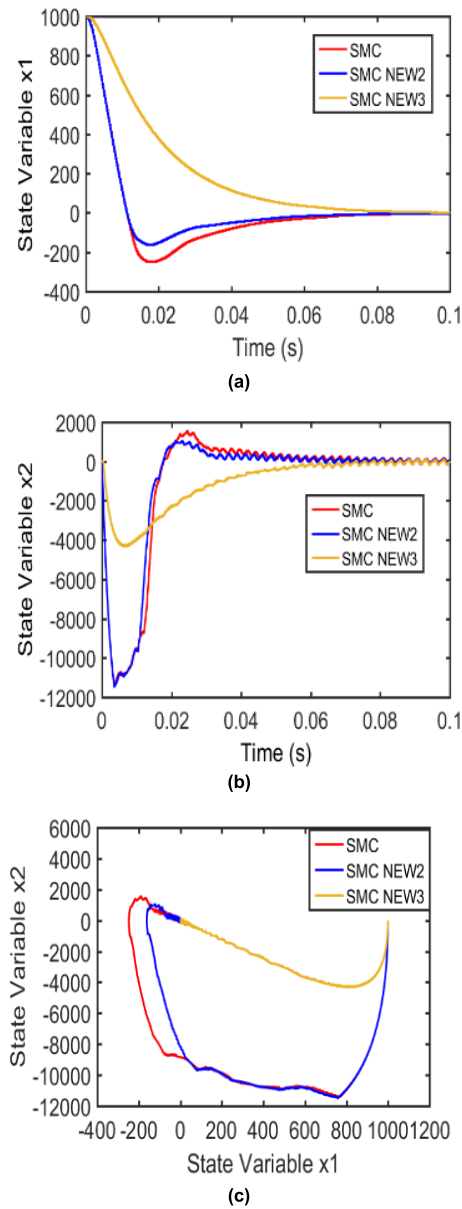


FIGURE 7. Comparison of the performance for other three reaching laws when $X = x_1$. (a) Reaching speed. (b) State convergence process. (c) Phase trajectory.

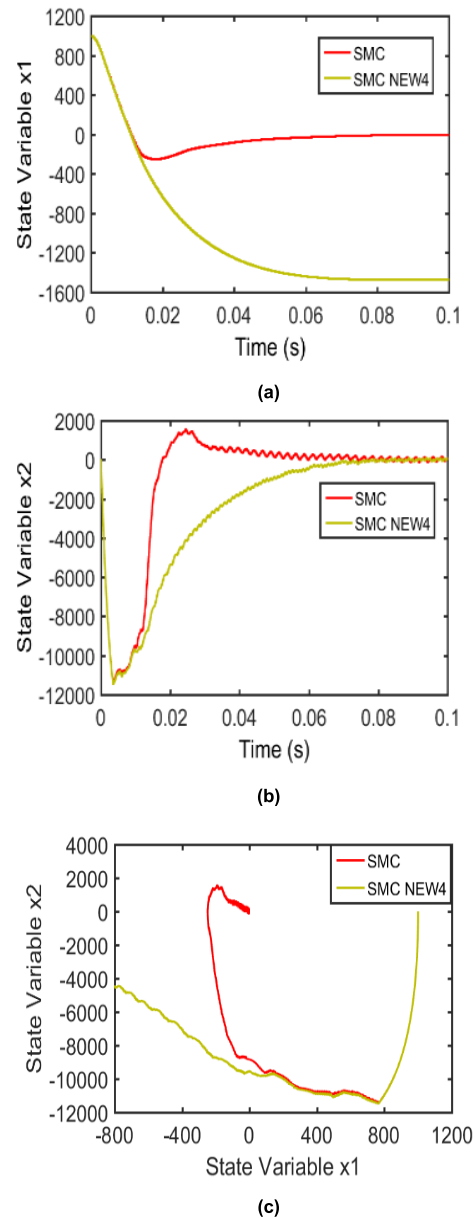


FIGURE 8. Comparison of the performance for two reaching laws when $X = x_2$ or s . (a) Reaching speed. (b) State convergence process. (c) Phase trajectory.

best choice to build the motor controller and for further application.

B. $X=x_2$ OR s

The reaching law at this time is as follows:

$$\begin{cases} \dot{s} = -m|x_2|^a \text{sign}(s) - qs \\ \dot{s} = -m|s|^a \text{sign}(s) - qs \end{cases} \quad \text{or} \quad (18)$$

In this situation, whatever X takes x_2 or s , and a takes a large or small value, the performance curves of this kind reaching law are all the same through the simulation. The reason why the above situation occurs may be that both x_2 and s

contain x_2 , x_2 is the derivative of x_1 and is a differential term, which may have a great impact on the system response.

The reaching law at this time is defined as ‘‘SMC NEW4’’ and its performance is shown in FIGURE 8. It can be seen from FIGURE 8. (a) and (c) that the system state cannot be stabilized at zero point, so this reaching law is not correct and suitable.

By synthesizing the proposed reaching laws in this section, we can draw a conclusion: After excluding the unreasonable reaching law (i.e. ‘‘SMC NEW4’’), ‘‘SMC NEW3’’ has the best reaching speed, state convergence process and the most regular phase trajectory, which can be regarded as the most suitable reaching law to apply in the motor control system.

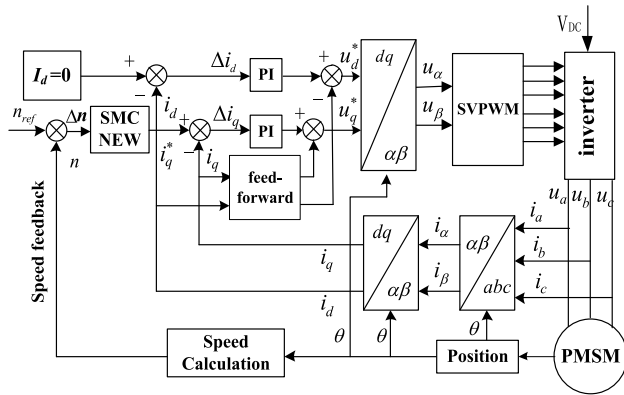


FIGURE 9. Control block diagram of sliding mode control system.

IV. SIMULATION AND CONTROL RESPONSES

In order to verify the effectiveness of the proposed control algorithm, a simulation model using three different reaching laws when $X = x_1$ (From the above section, we can know that the performance of the reaching laws at this time is better than the reaching law when $X = x_2$ or s), is established. Besides, to better illustrate the effectiveness of the novel method, the model of PI controller and overall system is also established and compared with three new reaching laws mentioned above.

Internal structure of the new sliding mode controller when $X = x_1$ is already displayed in FIGURE 3 (the red line). Also, the entire speed regulation system includes some other modules, such as:

Feed-forward compensation model—in order to eliminate the interaction between DQ -axes currents.

Coordinate transformation model—the amount of AC is converted to DC to simplify the calculation.

SVPWM—to form the PWM waveforms required by the inverter.

The control system block diagram is shown in FIGURE 9. The parameters of the studied PMSM are shown in TABLE 1. The simulation time is set to 0.3s; the motor’s given speed is set to 1000 r/min; the initial load torque is 0 N•m, and it is changed to 10N•m at 0.15s. Run the simulation and the system responses are shown in FIGURE 10-12 below.

The speed responses of three reaching laws and PI control algorithm coincide after nearly 0.08s, so do the torque responses; except for the fluctuation of the starting time, the trend of the current response curves are all the same. A detailed comparative analysis on above figures is performed, then the analysis results are given in the form of a table, as shown in TABLE 2.

We can get the following information from FIGURE 10-12 and TABLE 2:

- 1) Speed response: the comparison of the maximum fluctuation at the start time is: “PI>SMC>SMC NEW2>SMC NEW3”; the time to reach the steady state of all algorithms is fast; and when the load changes at 0.15s, all control methods can quickly return to the steady state.

TABLE 1. Modeling parameters of the studied PMSM.

Symbol	Parameter	Value
p	Number of pole pairs	4
R	Armature resistance	0.025 Ω
ϕ_f	PM flux linkage	0.062 Wb
L_d	D -axis inductance	0.20 mH
L_{eq}	Rated Q -axis inductance	0.47 mH
J	Moment of inertia	0.003 kg•m ²
P_N	Rated power	7.5 kW
I_N	Rated current	46.5 A
n_N	Rated speed	1000 r/min

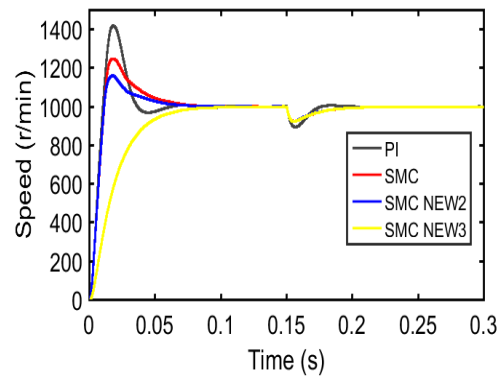


FIGURE 10. Comparison of speed responses between three different reaching laws when $X = x_1$ and PI control algorithm.

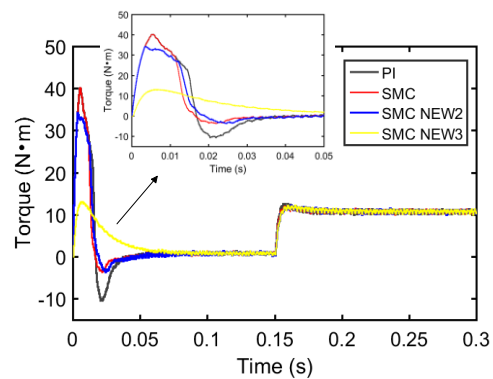


FIGURE 11. Comparison of torque responses between three different reaching laws when $X = x_1$ and PI control algorithm.

- 2) Torque response: the maximum fluctuations of “PI” and “SMC” are almost the same, but that of “SMC NEW2” is about 35N•m and that of “SMC NEW3” is about 13N•m, so “SMC NEW3” is the best one.

- 3) Phase current response: the relationship of the maximum fluctuation among different strategies are the same as that of torque response.

The “robustness” is a performance index of the control system. For motors, it refers to the characteristic of the drive

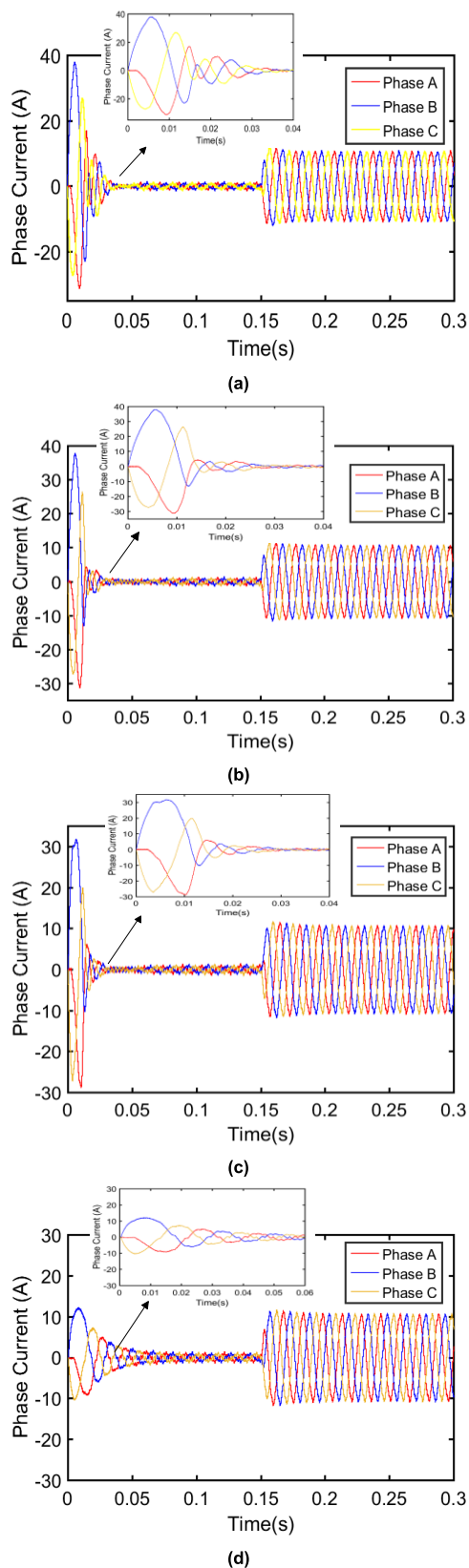


FIGURE 12. Comparison of phase current responses between three different reaching laws when $X = x_1$ and PI control algorithm. (a) PI. (b) SMC. (c) SMC NEW2. (d) SMC NEW3.

TABLE 2. Comparison of the system responses between three different reaching laws and PI control algorithm.

Control algorithm	Speed response maximum fluctuation	Torque response maximum fluctuation	Phase current response maximum fluctuation
PI	> 1400 r/min	$\approx 40\text{N}\cdot\text{m}$	$\approx 38\text{A}$
SMC	> 1200 r/min & < 1400 r/min	$\approx 40\text{N}\cdot\text{m}$	$\approx 38\text{A}$
SMC NEW2	< 1200 r/min	$\approx 35\text{N}\cdot\text{m}$	$\approx 30\text{A}$
SMC NEW3	0	$\approx 13\text{N}\cdot\text{m}$	$\approx 12\text{A}$

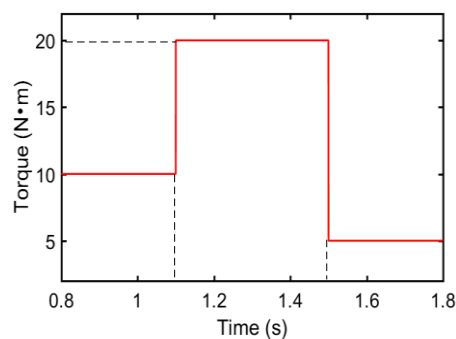


FIGURE 13. Variation of the load torque.

system to maintain its original performance under the perturbation of certain parameters. That is, the robustness of the system is the key to survive in abnormal situations such as the situation where large disturbances exist.

Therefore, after the motor is running smoothly, we add or reduce the load suddenly to observe whether the motor can return to the stable operation state, and then judge the robustness of the system. Similarly, we still compare four algorithms described above. The original load torque is $10\text{N}\cdot\text{m}$, the load torque increases to $40\text{N}\cdot\text{m}$ at 1.1s, and decreases to $5\text{N}\cdot\text{m}$ at 1.5s, as shown in FIGURE 13.

The variations of speed and output torque are shown in FIGURE 14 and 16, respectively. For a clearer analysis of the figures, the rectangular areas in the two pictures are enlarged as shown in FIGURE 15 and 17. We can get the following information from these four figures:

- 1) The variation of the actual motor speed of “SMC NEW2” is identical with that of “SMC NEW3”, so these two algorithms are collectively called “SMC NEW”.
- 2) Actual motor speed: from FIGURE 14 and 15, whether the load is increased or reduced, the relationship of the speed fluctuation is always: “PI> SMC> SMC NEW”.
- 3) Output Torque: from FIGURE 16 and 17, whether the load is increased or reduced, the relationship of the output torque fluctuation is same as that of the motor speed.

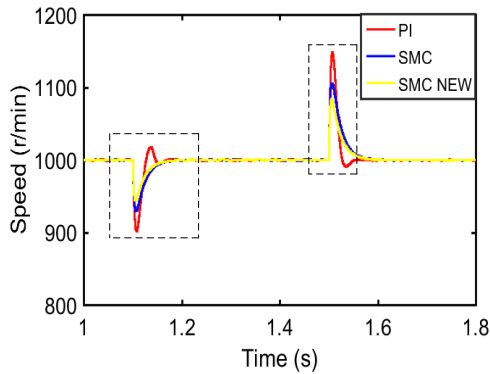


FIGURE 14. Variation of the actual motor speed along with the variation of the load torque.

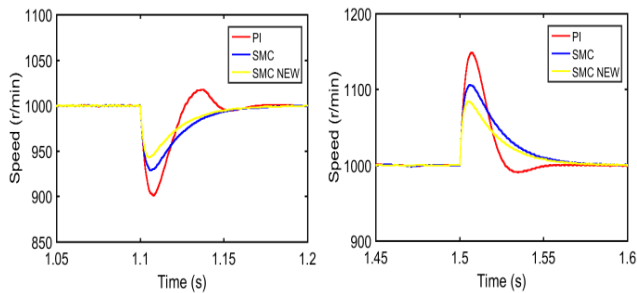


FIGURE 15. Partial enlargement of the actual motor speed.

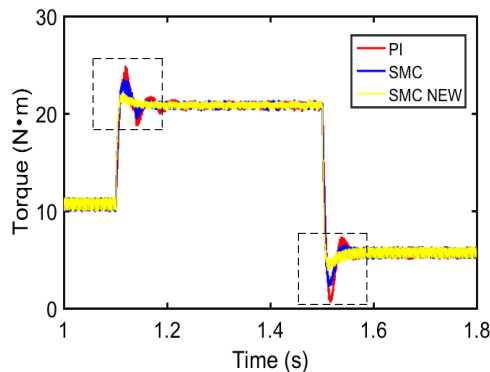


FIGURE 16. Variation of the output motor torque along with the variation of the load torque.

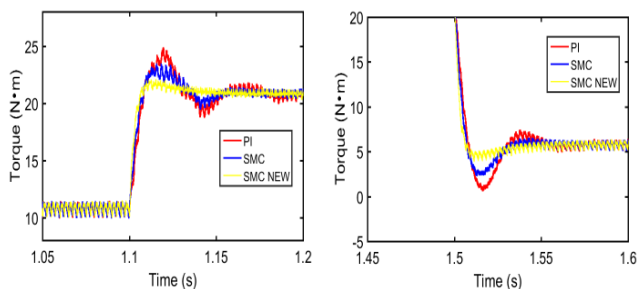


FIGURE 17. Partial enlargement of the output motor torque.

All of above figures and analysis indicate that the motor control system using improved exponential reaching law has a strong anti-disturbance ability, that is, a strong robustness.

Through a comprehensive analysis of the responses between different reaching laws and PI control strategy, the results are obvious that the performance of “SMC NEW2” and “SMC NEW3” are both improved compared with the original reaching law. Among them, the speed response of “SMC NEW3” will smoothly transit from zero to the steady state which has no speed fluctuation in the start-up stage of the motor; and the fluctuations of torque and current responses are all the smallest among the three proposed laws. Although the time for the current to reach the steady state is slightly increased, it has little effect on the system. In addition, the improved reaching laws have less fluctuation when the load changes, so their robustness is very strong.

In summary, the improved reaching laws is useful and “SMC NEW3” can be considered as the most suitable reaching law to apply in the control system for PMSM drive.

V. CONCLUSION

To solve the problem of magnetic saturation which has a serious influence on the performance of the PMSM drive system in practical application, an improved sliding mode control strategy based on exponential reaching law is proposed. The main work of this paper are as follows:

- (1) Mathematical model of PMSM considering magnetic saturation is established and the varying Q -axis inductance is applied into the system to reduce the error.
- (2) An improved reaching law is proposed to effectively improve the performance of the drive system. The intrinsic properties of these reaching laws are analyzed to explain whether they are suitable for application.
- (3) Use suitable reaching laws to build the new controller, run the simulation, and a comprehensive analysis is made. The results show that the improved exponential reaching law, especially “SMC NEW3” (i.e. $\dot{s} = -m |x_1|^3 \text{sign}(s) - qs$) has the best performance of the system responses, so the correctness and effectiveness of the proposed algorithm are verified. It is regarded as the most appropriate reaching law to be used in the PMSM drive system.

REFERENCES

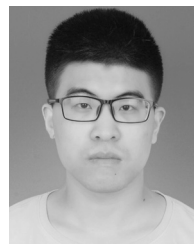
- [1] A. Masmoudi and Z.-Q. Zhu, “Fractional slot permanent magnet brushless machines and drives for electric and hybrid propulsion systems,” *COMPEL-Int. J. Comput. Math. Elect. Electron. Eng.*, vol. 30, no. 1, pp. 9–31, 2011.
- [2] T. M. Jahns, G. B. Kliman, and T. W. Neumann, “Interior permanent-magnet synchronous motors for adjustable-speed drives,” *IEEE Trans. Ind. Appl.*, vol. IA-22, no. 4, pp. 738–747, Jul. 1986.
- [3] Y.-S. Han, J.-S. Choi, and Y.-S. Kim, “Sensorless PMSM drive with a sliding mode control based adaptive speed and stator resistance estimator,” *IEEE Trans. Magn.*, vol. 36, no. 5, pp. 3588–3591, Sep. 2000.
- [4] M. K. Sarkar, Arkdev, and S. S. K. Singh, “Sliding mode control: A higher order and event triggered based approach for nonlinear uncertain systems,” in *Proc. 8th Annu. Ind. Automat. Electromech. Eng. Conf. (IEMECON)*, Bangkok, Thailand, Aug. 2017, pp. 208–211.
- [5] J. Leng and C. Ma, “Sliding mode control for PMSM based on a novel hybrid reaching law,” in *Proc. 37th Chin. Control Conf. (CCC)*, Wuhan, China, Jul. 2018, pp. 3006–3011.
- [6] T. Mizoshiri and Y. Mori, “Sliding mode control with a linear sliding surface that varies along a smooth trajectory,” in *Proc. SICE Int. Symp. Control Syst. (ISCS)*, Nagoya, Japan, Mar. 2016, pp. 1–6.

- [7] V. I. Utkin and K. D. Yang, "Methods for constructing discontinuity planes in multidimensional variable structure systems," *Automat. Remote Control*, vol. 31, no. 10, pp. 72–77, 1978.
- [8] A. Y. Sivaramakrishnan, M. V. Hariharan, and M. C. Srisailam, "Design of variable-structure load-frequency controller using pole assignment technique," *Int. J. Control*, vol. 40, no. 3, pp. 487–498, 1984.
- [9] D. Zhu and Y. Chai, "Tracking control of multi-linked robots based on terminal sliding mode," in *Proc. 30th Chin. Control Conf.*, Yantai, China, Jul. 2011, pp. 2539–2543.
- [10] X. Liu, H. Yu, J. Yu, and L. Zhao, "Combined speed and current terminal sliding mode control with nonlinear disturbance observer for PMSM drive," *IEEE Access*, vol. 6, pp. 29594–29601, 2018.
- [11] S. Yu and X. Yu, "Robust global fast terminal sliding mode controller for rigid robotic manipulators," in *Proc. IEEE Region 10 Conf. Comput., Commun., Control Power Eng. (TENCOM)*, Beijing, China, vol. 3, Oct. 2002, pp. 1335–1338.
- [12] Y. Feng, X. Yu, and Z. Man, "Non-singular terminal sliding mode control and its application for robot manipulators," in *Proc. IEEE Int. Symp. Circuits Syst.*, Sydney, NSW, Australia, vol. 2, May 2001, pp. 545–548.
- [13] F. Castanos and L. Fridman, "Analysis and design of integral sliding manifolds for systems with unmatched perturbations," *IEEE Trans. Autom. Control*, vol. 51, no. 5, pp. 853–858, May 2006.
- [14] P. Mani, R. Rajan, L. Shanmugam, and Y. H. Joo, "Adaptive fractional fuzzy integral sliding mode control for PMSM model," *IEEE Trans. Fuzzy Syst.*, vol. 27, no. 8, pp. 1674–1686, Aug. 2019.
- [15] S.-Z. Zhang and X.-I. Ma, "A PMSM sliding-mode control system based on exponential reaching law," in *Proc. Int. Conf. Comput. Aspects Social Netw.*, Taiyuan, China, Sep. 2010, pp. 412–414.
- [16] Y. Huang and H. Wang, "Torque balance of double motors drive system based on exponential reaching law VSSMC," in *Proc. 21st Int. Conf. Elect. Mach. Syst. (ICEMS)*, Jeju, South Korea, Oct. 2018, pp. 2771–2776.
- [17] H. Ma, J. Wu, and Z. Xiong, "A novel exponential reaching law of discrete-time sliding-mode control," *IEEE Trans. Ind. Electron.*, vol. 64, no. 5, pp. 3840–3850, May 2017.
- [18] G. Bartolini, A. Ferrara, and E. Usai, "Chattering avoidance by second-order sliding mode control," *IEEE Trans. Autom. Control*, vol. 43, no. 2, pp. 241–246, Feb. 1998.
- [19] A. Levant, "Construction principles of output-feedback 2-sliding mode design," in *Proc. 41st IEEE Conf. Decis. Control*, Las Vegas, NV, USA, vol. 1, Dec. 2002, pp. 317–322.
- [20] A. Levant, "Homogeneity approach to high-order sliding mode design," *Automatica*, vol. 41, no. 5, pp. 823–830, May 2005.
- [21] L. Chen, M. Liu, X. Huang, S. Fu, and J. Qiu, "Adaptive fuzzy sliding mode control for network-based nonlinear systems with actuator failures," *IEEE Trans. Fuzzy Syst.*, vol. 26, no. 3, pp. 1311–1323, Jun. 2018.
- [22] T. Wang and J. Fei, "Adaptive neural control of active power filter using fuzzy sliding mode controller," *IEEE Access*, vol. 4, pp. 6816–6822, 2016.
- [23] W.-J. Chang, P.-H. Chen, and C.-C. Ku, "Mixed sliding mode fuzzy control for discrete-time non-linear stochastic systems subject to variance and passivity constraints," *IET Control Theory Appl.*, vol. 9, no. 16, pp. 2369–2376, Oct. 2015.
- [24] T. Yang, N. Sun, H. Chen, and Y. Fang, "Neural network-based adaptive antisming control of an underactuated ship-mounted crane with roll motions and input dead zones," *IEEE Trans. Neural Netw. Learn. Syst.*, to be published.
- [25] A. Mishra, J. Makwana, P. Agarwal, and S. P. Srivastava, "Mathematical modeling and fuzzy based speed control of permanent magnet synchronous motor drive," in *Proc. 7th IEEE Conf. Ind. Electron. Appl. (ICIEA)*, Singapore, Jul. 2012, pp. 2034–2038.
- [26] Z. S. Wu, L. C. Zhang, and C. L. Zhao, "Adaptive controller and its application in force of asymmetric cylinder controlled by symmetric valve," *Chin. J. Mech. Eng.*, vol. 20, no. 6, pp. 50–53, 2007.
- [27] Y. Fang, X. F. Zhou, and X. Y. Zhang, "Sliding mode variable structure control of IPMSM speed control system based on new approach law and hybrid speed controller," *J. Elect. Eng.*, vol. 32, no. 5, pp. 9–18, Mar. 2017.



AIMENG WANG received the B.S. degree in electrical engineering from the Hebei University of Technology, China, in 1985, and the M.S. and Ph.D. degrees in electrical engineering from North China Electric Power University, Baoding, China, in 1999 and 2010, respectively, where she is currently a Professor with the School of Electrical Engineering.

She was a Visiting Professor with the Institute of Electrical Machines and Power Electronics, University of Wisconsin–Madison, USA, from January 2006 to 2007. She has published over 30 research articles and more than 10 scientific research projects are under research or completed. She has international cooperation and exchange projects with famous foreign universities for a long time. Her current research interests include permanent magnet synchronous machine design and its control for hybrid electric vehicle and for wind power system application.



SHENGJUN WEI received the B.S. degree in electrical engineering from the Hebei University of Science and Technology, China, in 2017. He is currently pursuing the M.S. degree in electric engineering with North China Electric Power University. His current research interest includes the design and control of the fractional slot centralized winding permanent magnet motor.

...